Magnetoelastic parametric instabilities of localized spin waves induced by traveling elastic waves

Ivan Lisenkov,* Albrecht Jander, and Pallavi Dhagat
School of Electrical Engineering and Computer Science, Oregon State University, Corvallis, Oregon 97331, USA

(Received 17 March 2019; published 24 May 2019)

A theory of parametric interaction between spin waves localized in a waveguide and traveling elastic waves is developed for ferromagnetic thin films. The presented theoretical formalism takes into account an arbitrary spatial distribution of the displacement field in the acoustic waves and an arbitrary magnetization in spin waves. Using the theory, we examine interaction of forward-volume spin waves (FVSW) localized in a narrow waveguide and Rayleigh surface acoustic waves traveling in a substrate underneath the waveguide. We show that, in contrast to classical electromagnetic pumping, the symmetry of the magnetoelastic interaction allows for the generation of first-order parametric instabilities in spin waves with circular precession, such as FVSW. At the same time the localization of spin waves modifies the momentum conservation law for the parametric process to include the transfer of momentum to the waveguide, which allows for a frequency separation of the interacting counterpropagating spin waves. The frequency separation enables amplification of a localized spin wave without generation of a traveling idler wave, which results in a greater amplification efficiency.

DOI: 10.1103/PhysRevB.99.184433

I. INTRODUCTION

Parametric interaction of waves has been studied in a broad range of physical systems, e.g., in nonlinear optics [1], plasma physics [2], acoustics [3], and magnetism [4] (for a review see Ref. [5]). The first-order parametric interaction (or three-wave processes) in bulk media manifests itself in the energy and momentum conservation laws [5]. The conservation laws define selection rules constraining which waves can parametrically interact. By Noether's theorem, the conservation of momentum derives from space-translational symmetry. If the translational symmetry is broken, i.e., if the area of the parametric interaction is limited in space [6], the global momentum conservation law allows transfer of momentum from the interacting waves to the confining structure, analogous to the radiation pressure effect [7]. As a consequence of the symmetry breaking, the selection rules for parametrically interacting waves are relaxed. For example, a localized electromagnetic pump allows parametric interaction of copropagating spin waves, while such interaction is not possible in the case of uniform pumping [6].

The translational symmetry is broken when the interacting waves are localized in potential wells or waveguides. The fact that the waves can propagate only in the directions allowed by the waveguides is reflected in the momentum conservation law for these waves. Since these momentum conservation conditions are different from the bulk case, the wave localization opens an additional degree of freedom for fine tuning of the parametric interaction. As an example of such a system, in this work we study the parametric interaction of spin waves, localized in a waveguide made of a magnetostrictive ferromagnet, with traveling *elastic* waves [8–11].

The parametric pumping of spin waves in thin ferromagnetic films by electromagnetic fields has been well studied [4,6,12–17] and has been shown to be useful for sustaining and amplifying spin-wave amplitudes. The nonlinear processes of magnetic parametric pumping have also been shown to find applications in analog signal processing [17].

The electromagnetic parametric pumping process is based on the Zeeman interaction between the oscillating magnetic field (typically in the microwave frequency range) and the time-varying component of magnetization parallel to the equilibrium magnetization. This is conventionally termed "parallel pumping" since the pumping magnetic field is parallel to the magnetization. In this geometry, the coupling between the spin waves' modes and the pumping field depends on the precession ellipticity [12] and vanishes for the spin waves with a circular precession. Therefore, the parallel pumping works well for backward-volume spin waves (BVSWs) in thin films, where the wave vector is parallel to the in-plane equilibrium magnetization and the thin-film shape anisotropy results in elliptical precession. However, the dispersion of BVSWs is not a single-valued function of the frequency [12], leading to instabilities for short and slow dipolar-exchange spin waves [6]. These dipolar-exchange spin waves are usually not usable in signal processing [16] because their wavelengths are too short to pick up with conventional spin-wave antennas. Forward-volume spin waves (FVSWs) propagate when the film is magnetized perpendicular to its plane. FVSWs have a single-valued dispersion function [12], but since the magnetization precession is circular in the long-wavelength limit, they cannot be pumped electromagnetically.

The mechanism of acoustic parametric pumping is different. The energy of spin-wave excitations depends on the magnetic anisotropy. Thus, in general, by modulating the magnetic

*Present address: Winchester Technologies, LLC, Burlington, Massachusetts 01803, USA; https://www.lisenkov.com; ivan@lisenkov.com

anisotropy one can parametrically interact with spin waves. In magnetostrictive materials, the magnetic anisotropy can be modulated via the magnetoelastic interaction by deformation of the sample. The energy of the magnetoelastic interaction is quadratic in the magnetization [see (8) below], in contrast to the energy of Zeeman interaction, which is linear with the magnetization. The form of the magnetoelastic energy allows, in particular, pumping of spin-wave modes with a circular precession. The parametric pumping of spin waves by traveling acoustic waves has been examined both experimentally and theoretically in bulk magnetostrictive media [8–11] and in infinitesimally thin films [18]. Recently, the parametric pumping of BVSWs by bulk acoustic waves was demonstrated in ferromagnetic films [19], proving the feasibility of spin-wave parametric pumping via magnetostriction. We note here that elastic waves have also been successfully employed to excite ferromagnetic resonance and traveling spin waves in a linear regime [20–22].

Typical dimensions of spin-wave devices employing electromagnetic pumping are much smaller than the electromagnetic wavelength; thus, the phase of the pumping electromagnetic field is practically uniform across the pumping region. Therefore, the pumping electromagnetic waves are always "seen" as being stationary by spin waves [6,15]. On the other hand, the wavelengths of acoustic waves are on the same order as typical spin-wave localization in modern magnonic and spintronic devices [16,23–26]. The small wavelength of the acoustic waves allows for studying parametric pumping of spin waves by traveling waves.

In this work, we develop a general theory of parametric interaction of acoustic waves and *localized* spin waves with arbitrary distribution of the displacement field in the acoustic wave and an arbitrary spin-wave mode. Employing the theory, we show a possibility of parametric instabilities in FVSWs, confined in a spin-wave waveguide, generated by Rayleigh surface acoustic waves (SAWs). The instabilities can be either convective or absolute for oblique or normal incidence of the SAW, respectively. The absolute instability leads to generation of FVSWs by SAWs. For convective instability, by selecting a critical incident angle one can achieve a regime where spin waves are amplified without generating a counterpropagating wave (idler), increasing the amplification efficiency. In yttrium iron garnet (YIG), a commonly used magnetostrictive ferrimagnet, the thresholds of the SAW strain amplitude for convective and absolute instabilities are less than ≈ 45 ppm, which is within the maximum experimentally achievable strain [27].

II. PARAMETRIC COUPLING BETWEEN ACOUSTIC AND SPIN WAVES

Theories for parametric magnetoelastic interactions [18,28,29] developed in the past focused on waves in bulk samples; that is, the localization of spin waves was not considered. Here we develop a theory that captures the physics of parametric interactions in a case of localized spin waves in samples with an arbitrary direction of the magnetization and acoustic wave modes with an arbitrary distribution of the strain field.

At first, we consider the dynamics of magnetization vector $\boldsymbol{M}(t,\boldsymbol{r})$ in a ferromagnetic sample without any deformation. This dynamics is governed by the Landau-Lifshitz equation [12]:

$$\frac{d\boldsymbol{M}(t,\boldsymbol{r})}{dt} = \gamma \boldsymbol{B}^{\rm eff}(t,\boldsymbol{r}) \times \boldsymbol{M}(t,\boldsymbol{r}), \tag{1}$$

where γ the gyromagnetic ratio and $\boldsymbol{B}^{\rm eff}$ is an effective magnetic field acting on the sample, including bias fields, shape, and crystalline anisotropy. Restricting analysis to small-angle precession dynamics (nonlinear terms can be added later in the same fashion as in [30]), we expand the magnetization $\boldsymbol{M}(t,\boldsymbol{r})$ to the static and dynamic parts:

$$\boldsymbol{M}(t,\boldsymbol{r}) = M_s[\boldsymbol{\mu}(\boldsymbol{r}) + \boldsymbol{s}(t,\boldsymbol{r})], \tag{2}$$

where M_s is the saturation magnetization, $\boldsymbol{\mu}(\boldsymbol{r})$ is the unit vector pointing in the direction of equilibrium magnetization (ground-state vector), and $\boldsymbol{s}(t,\boldsymbol{r})$ is the spin-wave excitation vector. In the absence of high-order anisotropy, the Landau-Lifshitz equation can be linearized by substituting (2) into (1) [12,30–33]:

$$\hat{\boldsymbol{J}}(\boldsymbol{r}) \cdot \frac{d\boldsymbol{s}(t,\boldsymbol{r})}{dt} = \int \hat{\boldsymbol{\Omega}}(\boldsymbol{r},\boldsymbol{r}') \cdot \boldsymbol{s}(t,\boldsymbol{r}') d^3\boldsymbol{r}', \tag{3}$$

where $\hat{\boldsymbol{J}}(\boldsymbol{r}) = \hat{\boldsymbol{e}} \cdot \boldsymbol{\mu}(\boldsymbol{r})$ is the angular momentum operator removing all components parallel to the static magnetization direction which are irrelevant to the magnetization dynamics, $\hat{\boldsymbol{e}}$ is the Levi-Civita operator, $\hat{\boldsymbol{\Omega}}(\boldsymbol{r},\boldsymbol{r}')$ is the Hamiltonian expressed in the frequency units of energy [30–32],

$$\hat{\boldsymbol{\Omega}}(\boldsymbol{r},\boldsymbol{r}') = \gamma B \hat{\boldsymbol{I}} \delta(\boldsymbol{r}-\boldsymbol{r}') + \gamma \hat{\boldsymbol{P}}(\boldsymbol{r}) \cdot \hat{\boldsymbol{\mathcal{D}}}(\boldsymbol{r},\boldsymbol{r}') \cdot \hat{\boldsymbol{P}}(\boldsymbol{r}'), \tag{4}$$

$\hat{\boldsymbol{\mathcal{D}}}(\boldsymbol{r},\boldsymbol{r}')$ is the self-adjoint operator describing the self-interactions in the ferromagnet *without any deformations*, $\hat{\boldsymbol{P}}(\boldsymbol{r}) = -\hat{\boldsymbol{J}}(\boldsymbol{r}) \cdot \hat{\boldsymbol{J}}(\boldsymbol{r})$ is the projector, and $\hat{\boldsymbol{I}}$ is an identity matrix. The modulus of the internal magnetic field B and the ground-state vector $\mu(\boldsymbol{r})$, entering (3), can be found from the "static" part of the Landau-Lifshitz equation:

$$\boldsymbol{\mu}(\boldsymbol{r}) B = \boldsymbol{B}^{\rm ext}(\boldsymbol{r}) - \int \hat{\boldsymbol{\mathcal{D}}}(\boldsymbol{r},\boldsymbol{r}') \cdot \boldsymbol{\mu}(\boldsymbol{r}') d^3\boldsymbol{r}'. \tag{5}$$

See the Supplemental Material in Ref. [30] for more details of this formalism. Additionally, higher-order anisotropy terms can be introduced in a manner similar to that in [31].

Here Eq. (3) is a generalized eigenvalue problem; thus, its solutions can be written as

$$\boldsymbol{s}(t,\boldsymbol{r}) = \sum_\nu c_\nu e^{-i\omega_\nu t} \boldsymbol{s}_\nu(\boldsymbol{r}) + \text{c.c.}, \tag{6}$$

where c_ν is the dimensionless complex amplitude of the νth mode. Here the eigenmodes $\boldsymbol{s}_\nu(\boldsymbol{r})$ form an orthogonal basis with an orthogonality condition [30,33]:

$$\int \boldsymbol{s}_\nu^\dagger(\boldsymbol{r}) \cdot \hat{\boldsymbol{J}}(\boldsymbol{r}) \cdot \boldsymbol{s}_{\nu'}(\boldsymbol{r}) d^3\boldsymbol{r} = -i\mathcal{A}_\nu \delta_{\nu\nu'}, \tag{7}$$

where $\mathcal{A}_\nu > 0$ is the mode norm, $\dagger$ denotes Hermitian conjugation, and $\delta_{\nu,\nu'}$ is the Kronecker delta.

Deformation of a magnetic material changes the energy density $\mathscr{W}$ of the magnetic subsystem by the value

$$\mathscr{W}_{\mathrm{me}}(t,\boldsymbol{r}) = \frac{1}{M_s^2} b_{ijkl} U_{ij}(t,\boldsymbol{r}) \boldsymbol{M}_k \boldsymbol{M}_l, \tag{8}$$

where $U_{ij}(t,\boldsymbol{r})$ is the induced strain, b_{ijkl} is the tensor of magnetostriction, $ijkl = \{x,y,z\}$, and repetitive indices indicate summation. The effect of the strain can be introduced into (3)–(5) as a perturbation to the self-interaction operator

$$\begin{aligned}\delta\hat{\boldsymbol{\mathcal{D}}}(t,\boldsymbol{r},\boldsymbol{r}') &= \frac{2}{M_s} b_{ijkl} U_{ij}(t,\boldsymbol{r}) \delta(\boldsymbol{r}-\boldsymbol{r}')\\ &= a(t)\hat{\boldsymbol{T}}(\boldsymbol{r})\delta(\boldsymbol{r}-\boldsymbol{r}') + \text{c.c.},\end{aligned} \tag{9}$$

where $U_{ij}(t,\boldsymbol{r}) = a(t)u_{ij}(\boldsymbol{r}) + \text{c.c.}$, $a(t)$ and $u_{ij}(\boldsymbol{r})$ are the dimensionless complex amplitude and the complex mode profile of the acoustic wave, and $\hat{\boldsymbol{T}}(\boldsymbol{r}) = 2b_{ijkl}u_{ij}(\boldsymbol{r})/M_s$. Here the operator $\hat{\boldsymbol{T}}(\boldsymbol{r})$ can be seen as a tensor for an effective magnetic anisotropy generated by the acoustic field. Substituting the perturbation (9) into (5) and multiplying by $\boldsymbol{\mu}(\boldsymbol{r})$, we find the time-dependent correction to the internal magnetic field (we assume that the strain has no static component):

$$\delta B(t,\boldsymbol{r}) = -a(t)\boldsymbol{\mu}(\boldsymbol{r}) \cdot \hat{\boldsymbol{T}}(\boldsymbol{r}) \cdot \boldsymbol{\mu}(\boldsymbol{r}) + \text{c.c.} \tag{10}$$

Adding perturbation to (3) leads to

$$\begin{aligned}&\hat{\boldsymbol{J}}(\boldsymbol{r}) \cdot \frac{d\boldsymbol{s}(t,\boldsymbol{r})}{dt}\\ &\quad = \int \hat{\boldsymbol{\Omega}}(\boldsymbol{r},\boldsymbol{r}') \cdot \boldsymbol{s}(t,\boldsymbol{r}') d^3\boldsymbol{r}' + \gamma \delta B(t,\boldsymbol{r}) \boldsymbol{s}(t,\boldsymbol{r})\\ &\qquad + [a(t)\hat{\boldsymbol{T}}(\boldsymbol{r}) + \text{c.c.}] \cdot \boldsymbol{s}(t,\boldsymbol{r}) + [a(t)\hat{\boldsymbol{T}}(\boldsymbol{r}) \cdot \boldsymbol{\mu}(\boldsymbol{r}) + \text{c.c.}].\end{aligned} \tag{11}$$

We solve the perturbed equation (11) by substituting $\boldsymbol{s}(t,\boldsymbol{r}) = \sum_\nu c_\nu(t)\boldsymbol{s}_\nu(\boldsymbol{r}) + \text{c.c.}$ and multiplying by $\boldsymbol{s}^\dagger_{\nu'}(\boldsymbol{r})$. Using condition (7) and retaining only "parametric" terms [6], we obtain

$$\frac{dc_\nu(t)}{dt} + i\omega c_\nu(t) + \Gamma_\nu c_\nu(t) = a(t) \sum_{\nu'} V_{\nu\nu'} c^\dagger_{\nu'}(t), \tag{12}$$

where Γ_ν is the phenomenological damping term and $V_{\nu\nu'}$ is the coupling coefficient, which can be calculated as

$$\begin{aligned}V_{\nu\nu'} &= V^1_{\nu\nu'} + V^2_{\nu\nu'}\\ &= -i\frac{\gamma}{\mathcal{A}_\nu} \int [\boldsymbol{s}^\dagger_{\nu'}(\boldsymbol{r}) \cdot \boldsymbol{s}^\dagger_\nu(\boldsymbol{r})][\boldsymbol{\mu}(\boldsymbol{r}) \cdot \hat{\boldsymbol{T}}(\boldsymbol{r}) \cdot \boldsymbol{\mu}(\boldsymbol{r})] d^3\boldsymbol{r}\\ &\quad + i\frac{\gamma}{\mathcal{A}_\nu} \int [\boldsymbol{s}^\dagger_{\nu'}(\boldsymbol{r}) \cdot \hat{\boldsymbol{T}}(\boldsymbol{r}) \cdot \boldsymbol{s}^\dagger_\nu(\boldsymbol{r})] d^3\boldsymbol{r}.\end{aligned} \tag{13}$$

This expression is the central result of this work; it enables one to calculate the parametric coupling between arbitrary spin waves and acoustic waves. Using this result with the well-developed theory of parallel pumping [4,6,15,16], we can investigate the dynamics of spin waves under acoustic pumping.

The mode profiles in (13) [the distribution of magnetization $\boldsymbol{s}(\boldsymbol{r})$ for spin waves and the distribution of strain $\hat{\boldsymbol{u}}(\boldsymbol{r})$ for acoustic waves] can either be calculated analytically or extracted from numerical simulations for acoustic waves and spin waves. Importantly, we have not used an explicit form of the self-interaction operator $\hat{\boldsymbol{\mathcal{D}}}(\boldsymbol{r},\boldsymbol{r}')$. Thus, the presented theory is not restricted to a particular configuration of the problem, i.e., a direction of the equilibrium magnetization, a specific type of an acoustic wave, or a particular geometry of the magnetic sample, as was the case in previous methods [8,18,34,35].

We note also that a general expression similar to (13), but for linear magnetoelastic interactions, was obtained in Ref. [36].

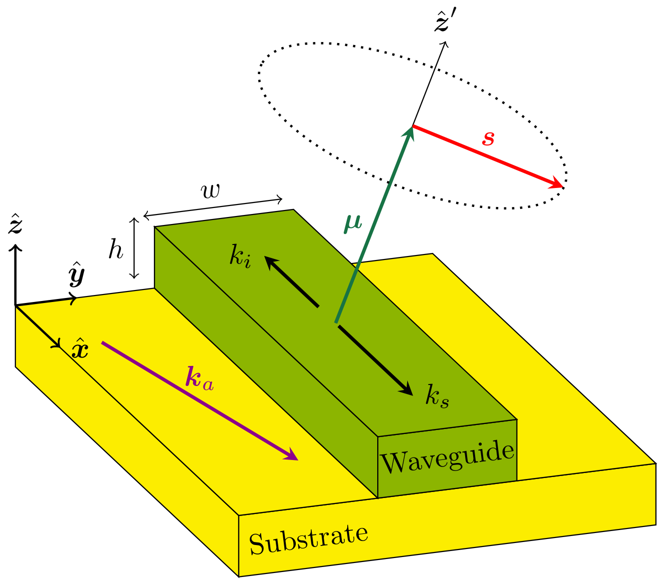

FIG. 1. Sketch showing the geometry of the confined spin-wave waveguide located on a substrate.

III. SELECTION RULES AND A MOMENTUM CONSERVATION LAW

To discuss the physical meaning of the terms entering the coupling coefficient $V_{\nu\nu'}$, we consider a simple case: a rectangular magnetic waveguide placed atop a solid nonmagnetic substrate (see Fig. 1). The waveguide is infinite in the $\hat{\boldsymbol{x}}$ direction and constrained in the $\hat{\boldsymbol{y}}$ and $\hat{\boldsymbol{z}}$ directions. The width of the waveguide is w, and the height is h. The magnetic waveguide is uniformly magnetized with the magnetic ground state $\boldsymbol{\mu}$.

The spin waves can travel along the x direction in the waveguide and are constrained in the y and z directions (see Fig. 1). In this situation we consider the interaction of three waves: two spin waves with wave numbers k_s and k_i (traditionally termed "signal" and "idler" waves) and an acoustic wave propagating in the x, y plane with wave vector $\boldsymbol{k}_a$ (see Fig. 1).

A spin excitation vector for each wave (signal and idler) can be written as

$$\boldsymbol{s}_k = \tilde{\boldsymbol{s}}_k f_k(y,z) e^{ikx}, \tag{14}$$

where $k = k_s, k_i,\ f_k(y,z)$ is the spin-wave mode profile across the waveguide, i.e., the distribution of the spin-wave mode amplitude within the waveguide, and $\tilde{\boldsymbol{s}}_k$ is the polarization of the spin-wave mode. The polarization $\tilde{\boldsymbol{s}}_k$ depends on the direction of the equilibrium magnetization $\boldsymbol{\mu}$ and ellipticity of precession. In a coordinate system where the z' axis is oriented with the equilibrium magnetization ($\boldsymbol{\mu} = \hat{z}'$) the polarization can be written as (see Fig. 1)

$$\tilde{\boldsymbol{s}}'_k = \begin{pmatrix} 1 \\ i\epsilon_k \\ 0 \end{pmatrix}, \tag{15}$$

where ϵ_k is the ellipticity of the precession. For simplicity we take the ellipticity to not depend on the spatial coordinates in the waveguide. The mode norm can be calculated as

$$\mathcal{A}_k = 2\epsilon_k \iint_S |f_k(y,z)|^2 dy dz = 2\epsilon_k \mathcal{A}_k^S, \tag{16}$$

where S is the cross-sectional area of the waveguide (see Fig. 1).

Let us also choose that the acoustic wave is uniform in the entire space and propagates in the plane of the waveguide,

$$u_{ij} = \tilde{u}_{ij} e^{i\boldsymbol{k}_a\cdot\boldsymbol{r}} = \tilde{u}_{ij} e^{i(k_{||}x + k_\perp y)}, \tag{17}$$

where $k_{||}$ and $k_\perp$ are the projections of the acoustic wave vector on the x and y axes, respectively.

Substituting the assumed mode profiles into (13), we have

$$V_{k_s,k_i} = \gamma \left(\tilde{V}^1_{k_s,k_i} + \tilde{V}^2_{k_s,k_i}\right) F_{k_s,k_i} \delta(k_s + k_i - k_{||}), \tag{18}$$

where

$$F_{k_s,k_i} = \frac{1}{\mathcal{A}^S_{k_s}} \iint_S f_{k_s}(y,z) f_{k_i}(y,z) e^{ik_\perp y} dy dz \tag{19}$$

is the overlap integral between two spin waves and one acoustic wave.

The δ function in (18) postulates a momentum conservation law:

$$k_s + k_i = k_{||}. \tag{20}$$

This conservation law is modified in the comparison to the bulk case [29], $\boldsymbol{k}_s + \boldsymbol{k}_i = \boldsymbol{k}_a$, i.e., when the spin waves are not localized in the waveguide. In the localized case the translational symmetry holds in the x direction and breaks in the y direction. Therefore, as a consequence of Noether's theorem, the x component of momentum is conserved for three interacting waves, but the y component is not. The momentum conservation law acts as a selection rule, defining the wave numbers of the interacting spin waves.

Expression (20) corresponds to the case of the electromagneticlike spin-wave pumping [4,6] when the acoustic wave has no x component $k_{||} = 0$ and to the "optical"-like copropagating wave pumping [1] for $\boldsymbol{k}_a = k_{||}\hat{\boldsymbol{x}}$.

The overlap integral F_{k_s,k_i} contains profiles of both spin waves and an oscillating function $e^{ik_\perp x}$. The overlap integral defines another selection rule for interacting spin waves based on the precession amplitude spatial distribution $f_{k_s}(y,z)$ and $f_{k_i}(y,z)$. In general, the calculation of mode spatial profiles is nontrivial and frequently requires numerical solutions. However, under reasonable assumptions we can analyze the behavior of the overlap integral analytically. If the cross-section distribution of both waves is uniform, $f_{k_s}(y,z) = f_{k_i}(y,z) = 1$, the overlap integral can easily be calculated as

$$F_{k_s,k_i} = \frac{\sin(k_\perp w/2)}{k_\perp w/2}. \tag{21}$$

From the above equation, one can conclude that the coupling coefficient drops with the width of the waveguide and the parametric interaction becomes inefficient when $w \gg 1/k_\perp$.

In the case of thin waveguides, $h \ll w$ (see Fig. 1), we can consider $f_k(y,z)$ to be harmonic functions depending on the y coordinate [37–39]. Here we consider two practically important cases, when the magnetization is pinned and unpinned at the waveguide boundaries in the y direction. Also, we assume that the profiles are identical for signal and idler waves, $f_{k_s}(y,z) = f_{k_i}(y,z) = f_k(y,z)$. Thus, the spatial profiles can be written as

$$f_k = \cos\left(\frac{\pi N(y + w/2)}{w}\right),$$
$$f_k = \sin\left(\frac{\pi N(y + w/2)}{w}\right) \tag{22}$$

for unpinned and pinned magnetization, respectively, where $N = 1, 2, \ldots$ is the mode number. Substituting the expressions for spatial profiles into (19), we find expressions for the overlap integral in two cases:

$$F^u_{kk} = \frac{4(2N^2\pi^2 - k_\perp^2 w^2)\sin(k_\perp w/2)}{4\pi^2 k_\perp w N^2 - k_\perp^3 w^3}, \tag{23}$$
$$F^p_{kk} = \frac{8N^2\pi^2 \sin(k_\perp w/2)}{4\pi^2 k_\perp w N^2 - k_\perp^3 w^3} \tag{24}$$

for unpinned and pinned magnetization, respectively. Similar to (21), these functions have a global maximum at $k_\perp w \to 0$. However, they also exhibit a local maximum at $w = 2\pi N/k_\perp$: $F^u_{kk} = F^u_{kk} = \pm 1/2$, allowing for interaction of high-order modes, $N > 0$, in wide waveguides $w > 1/k_\perp$.

Finally, we consider terms of $\tilde{V}^1_{k_s,k_i}$ and $\tilde{V}^2_{k_s,k_i}$. These terms define selection rules based on the vector structure of the magnetization precession, elastic deformations, and magnetostrictive tensor b_{ijkl}. The first term can be written in the form

$$\tilde{V}^1_{k_s,k_i} = -i\frac{1-\epsilon^2}{2\epsilon}\tilde{b}_p, \tag{25}$$

where we consider the ellipticity of both idler and signal spin waves to be identical, $\epsilon_{k_s} = \epsilon_{k_i} = \epsilon$. The term $\tilde{b}_p = \boldsymbol{\mu}\cdot\hat{\boldsymbol{T}}\cdot\boldsymbol{\mu}$, with $\hat{\boldsymbol{T}} = b_{ijkl}\tilde{u}_{ij}$, describes the projection of an effective magnetic field, generated by the inverse magnetostriction effect on the direction of the static magnetization. The symmetry of the term $\tilde{V}^1_{k_s,k_i}$ is identical to the symmetry of the coupling coefficient to an rf magnetic field for the parallel pumping mechanism [12]. Therefore, this term vanishes for a spin wave with circular precession, i.e., $\epsilon = 1$.

The second term, $V^2_{k_s,k_i}$, is different: Here the operator $\hat{\boldsymbol{T}}$ acts directly on the spin-wave mode profiles, and the coupling coefficient can be nonzero even for modes with circular precession:

$$\tilde{V}^2_{k_s,k_i} = i\frac{\boldsymbol{s}_{k_s}\cdot\hat{\boldsymbol{T}}\cdot\boldsymbol{s}_{k_i}}{2\epsilon_k}. \tag{26}$$

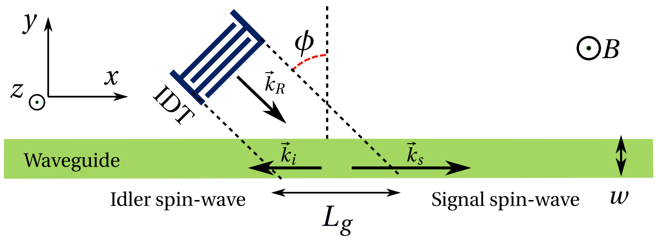

FIG. 2. Top view of a setup for spin-wave and surface acoustic wave parametric interaction. A Rayleigh surface acoustic wave excited, for example, by an interdigitated transducer (IDT), propagates in the substrate, while a spin wave propagates in the magnetic waveguide (green). The magnetic field $\boldsymbol{B}$ is applied perpendicular to the plane.

The particular form of this term depends on the deformation introduced by the acoustic wave and the symmetry of the tensor of magnetostriction. Physically, this term represents perturbations of the precession trajectory made by the modulation of the effective magnetic anisotropy. We note here that similar terms were obtained for the parametric pumping of spin waves with voltage-controlled magnetic anisotropy [40,41].

IV. INTERACTION BETWEEN SURFACE ACOUSTIC WAVES AND FORWARD-VOLUME SPIN WAVES

As an illustration of our theory, we calculate the parametric interactions between forward-volume spin waves traveling in a YIG waveguide and a Rayleigh SAW traveling in the gadolinium gallium garnet substrate (velocity $c_R \approx 5\,\mathrm{km/s}$; see Fig. 2). The parameters for YIG are taken as follows: Saturation magnetization [12] is $M_s = 135\,\mathrm{kA/m}$, exchange constant [42] $A_{\mathrm{ex}} = 3.7\,\mathrm{fJ/m}$, the magnetostrictive tensor components for a cubic crystal [12] $b_{iiii} = B_1 = 0.35\,\mathrm{MJ/m^3}$ and $b_{ijij} = B_2 = 0.7\,\mathrm{MJ/m^3}$, $i \neq j$, and the damping decrement $\Gamma/(2\pi) = \gamma\delta H/2 = 1.5\,\mathrm{MHz}$.

The calculation of the acoustic field in a YIG waveguide placed atop a substrate is nontrivial [34]. To simplify our analytical calculations, we will consider a thin and narrow ferromagnetic waveguide with $h \ll \lambda_R$ and $w < L_g$, where $\lambda_R = 2\pi k_R$ is the SAW wavelength, k_R is the SAW wave number, h is the thickness, w is the width, and L_g is the length of the interaction region (see Fig. 2). Also for simplicity, we assume that the strain is uniformly distributed in the waveguide and equal to the surface strain created by the SAW [43] and that the substrate is isotropic. Thus, the acoustic mode has the form $\hat{\boldsymbol{u}} = (\boldsymbol{k}_R \otimes \boldsymbol{k}_R/k_R^2 + iu_{zz}\boldsymbol{z} \otimes \boldsymbol{z})e^{i\boldsymbol{k}_R\cdot\boldsymbol{r}}$, where u_{zz} is the ratio between the vertical and lateral stresses. We also consider the pumping to be coherent in time as $a(t) = ae^{-i\omega_p t}$.

Spin-wave modes in perpendicular magnetized waveguides are typically pinned to the lateral edges. The spin excitation vector for the fundamental mode can be written as $\boldsymbol{s}_k = (\hat{\boldsymbol{x}} + i\epsilon_k\hat{\boldsymbol{y}})\sin(\pi y/w)e^{ikx-i\omega t}$, where ϵ is the precession ellipticity and the precession is almost circular ($|1 - |\epsilon_k|| \ll 1$) for perpendicularly magnetized samples and small k.

First, we consider the case of an infinitely long pumping region L_g. Using the above-described formalism in Sec. III in (13), we obtain expressions of the coupling coefficient between the signal and idler waves:

$$V_{k_s,k_i} = V_0(\phi) = \frac{\gamma B_1}{M_s}\frac{[\cos\phi - i\epsilon_k\sin(\phi)]^2 - iu_{zz}\left(1-\epsilon_k^2\right)}{2\epsilon_k} \times F_{kk}^p\delta(k_s + k_i - k_R\sin\phi) \approx \frac{\gamma B_1}{2M_s}F_{kk}^p\delta(k_s + k_i - k_R\sin\phi)e^{i\phi}. \tag{27}$$

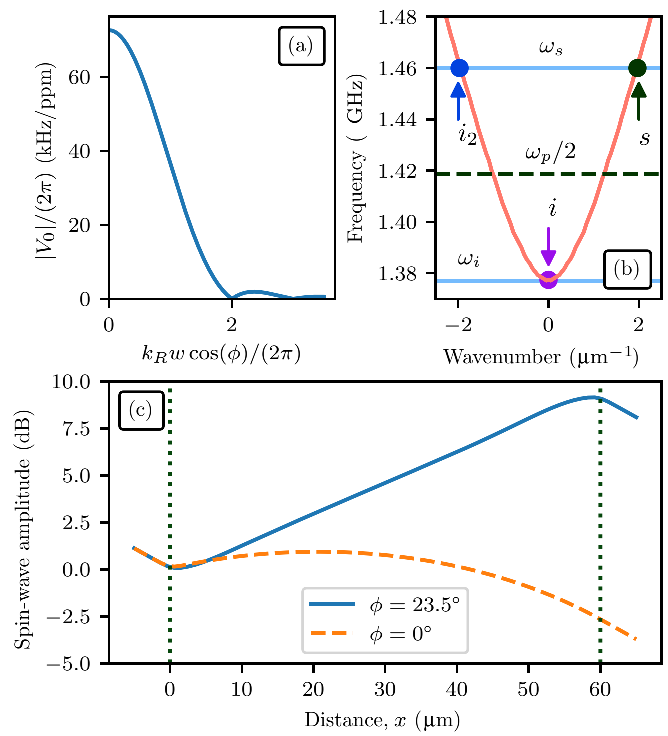

FIG. 3. (a) Parametric interaction coefficient V_0 for the surface acoustic waves and spin waves in a rectangular waveguide as a function of the waveguide width w and the projection of the SAW wave vector perpendicular to the waveguide $k_\perp$. (b) Numerically calculated spin-wave spectrum in a rectangular YIG waveguide. (c) Amplitude of spin waves under a parametric pumping for an obliquely (blue solid line) and normally (orange dashed line) incident SAW; vertical dotted lines enclose the pumping region. The amplitude of the strain in the acoustic wave is selected as $a = 31$ ppm $> a_{\mathrm{th}}(\phi)$. See text for the parameters of the waveguide and materials.

The factor $V_0(\phi)$ defines the "strength" of the parametric interaction. The modulus of $V_0(\phi)$ is plotted in Fig. 3(a) for parameters of YIG. A parametric instability in a waveguide with an infinitely long pumping region occurs when pumping overcomes the damping in the system. The threshold amplitude of the SAW is defined by the expression (assuming that ω_{k_s} and ω_{k_i} fall within the spin-wave spectra)

$$|a_{\mathrm{th}}(\phi)| = \Gamma/|V_0(\phi)|, \tag{28}$$

where Γ is the damping decrement of the fundamental mode. For $\phi = \pi/2$, i.e., when all three waves travel collinearly, the threshold value is equal to the threshold value obtained when ignoring the spin-wave localization [12,18]. For the selected parameters the threshold value is $|a_{\mathrm{th}}^{\mathrm{min}}| \approx 21\,\mathrm{ppm}$, which is lower than the typical failure strain (300 ppm) of Al transducers [27]. If $\phi \neq \pi/2$, the existence of the spin-wave localization increases the threshold for the spin-wave instability. The particular type of instability (absolute or convective, in other words, developing in time or space, respectively) is defined by the relative signs of the group velocities $\upsilon_{\mathrm{gr}}(k_s)$ and $\upsilon_{\mathrm{gr}}(k_i)$ [6].

The threshold (28) is directly proportional to the damping in the magnetic material and inversely proportional to the coefficient of magnetostriction. Therefore, it is feasible to consider materials with higher damping rates but, at the same time, stronger magnetoelastic interaction as a substitute for YIG. For example, recently, linear [44–46] and parametric [47] magnetoelastic interactions were observed in relatively lossy Ni films. Using (28) and parameters for Ni films [36] ($\alpha_G = 0.045$, $B_1 \approx B_2 \approx 10\,\mathrm{MJ/m^3}$, $\mu_0 M_s = 0.66\,\mathrm{T}$, $\omega/(2\pi) = 1.5\,\mathrm{GHz}$), we can estimate the strain threshold as $|a_{\mathrm{th,\,Ni}}^{\mathrm{min}}| \approx 260\,\mathrm{ppm}$, which is at the limit of the commonly used Al SAW transducers but easily obtainable with optical techniques of SAW excitation [46,48].

V. PARAMETRIC INSTABILITIES IN A SPATIALLY LIMITED PUMPING REGION

Experimentally, the pumping region is always limited in space. A localized pumping region increases the threshold for absolute instabilities and prevents the development of convective instabilities [15,49]. Absolute instabilities lead to generation of detectable spin waves from thermal fluctuations, which is often a problem in amplifiers and active delay lines, where the parasitic generation can cause undesired cross talk. On the other hand, a special case of convective instability when the group velocity of the idler wave becomes zero is important for spin-wave amplifiers. Since the idler then cannot "leak" outside the pumping region, the parametric interaction is very effective [49]. Such a situation is difficult to implement for electromagnetic pumping because the frequency and group velocities for both signal and idler spin waves are the same. For acoustic pumping, the modified momentum conservation law (20) allows parametric interaction of spin waves with different wave numbers and, as a consequence, with different frequencies, $\omega_{k_s} \neq \omega_{k_i}$ and $\omega_{k_s} + \omega_{k_i} = \omega_p$. To achieve a convective instability we select the idler wave with a zero group velocity $\upsilon_{\mathrm{gr}}(k_i) = 0$ at $k_i = 0$. Thus, for a signal wave with the frequency ω_{k_s} the pumping frequency is $\omega_p = \omega_{k_s} + \omega_{k_i=0}$, and $\sin\phi = k_s/k_R$.

In our example we take the waveguide with geometrical parameters $h = 100\,\mathrm{nm}$ and $w = 1\,\mu\mathrm{m}$, which can be fabricated experimentally [50], and the interaction region has length $L_g = 60\,\mu\mathrm{m}$ (see Fig. 2). The spin-wave spectrum in the waveguide biased by normal magnetic field $B = 20\,\mathrm{mT}$ is shown in Fig. 3(b). Since the waveguide is limited in the lateral direction, the spin-wave group velocity drops with the wave number approaching zero. The spectrum was calculated numerically using the MUMAX[3] micromagnetics simulator [51].

We select the signal frequency $\omega_{k_s}/(2\pi) = 1.46\,\mathrm{GHz}$, which corresponds to $k_s \approx 2\,\mu\mathrm{m}^{-1}$ [marked by the symbol s in Fig. 3(b)]. The spectrum minimum with $k = 0$ corresponds to the frequency $\omega_{k_i} = 1.37\,\mathrm{GHz}$ [symbol i in Fig. 3(b)]. To satisfy the conservation laws we select the pumping frequency $\omega_p \approx 2.48\,\mathrm{GHz}$ [see Fig. 3(b)]. To satisfy (20) we shall select an appropriate incident angle, $\phi_0 \approx 23.5^\circ$. The parametric coefficient for this angle is $\mathrm{V}_0(\phi_0) \approx 50\,\mathrm{kHz/ppm}$.

We use a standard "slow-envelope" technique to find the spin-wave amplitude distribution [4,6,15]. However, in our case, the group velocity of the idler spin waves vanishes; thus, we need to take into account the spin-wave diffusion of the idler waves [49]:

$$\begin{aligned} \upsilon_{\mathrm{gr}}\frac{db_s(x)}{dx} + \Gamma b_s(x) &= V_0\theta_P(x)b_i^\dagger(x)a, \\ i\frac{D}{2}\frac{d^2b_i^\dagger(x)}{dx^2} + \Gamma b_i^\dagger(x) &= -V_0^\dagger\theta_P(x)b_s(x)a, \end{aligned} \tag{29}$$

where $b_{s,i}(x)$ are the amplitudes of the signal and idler envelopes (see Ref. [15] for definition), $\upsilon_{\mathrm{gr}} \approx 0.38$ km/s is the group velocity of the signal wave, $D = d^2\omega_k/dk^2 \approx 2.24\,\mathrm{cm^2/s}$ is the diffusion coefficient, and $\theta_P(x)$ is a function which equals 1 inside the interaction region and 0 otherwise. The values of D and υ_{gr} were calculated numerically using MUMAX[3].

The amplitude of the signal wave found by a numerical solution of (29) is plotted in Fig. 3(c) with the blue line for the in-plane SAW strain amplitude $a_0 = 31\,\mathrm{ppm}$. This value is above the threshold (28), and the energy coming from the acoustic wave overcomes damping in the system. The amplitude of the signal and idler (not shown) waves exponentially increases in the $x > 0$ direction. The growth of the amplitude is limited by the finite length of the interaction region.

The induced idler wave can interact, in its turn, with a "secondary" idler wave with frequency ω_{k_s} and wave number $-k_s$, marked as i_2 in Fig. 3(b). This interaction, however, can be effective only in a nonadiabatic case [6], $k_sL_g \ll 1$. For the considered geometry this interaction is negligibly small.

The dashed orange line in Fig. 3(c) represents a solution for a normally incident SAW ($\phi = 0$). In this case both signal and idler waves have the same frequency [$\omega_p/2 \times 1/(2\pi) \approx 1.42$ GHz] and group velocity $\upsilon_{\mathrm{gr}} \approx 0.38$ km/s. In order to make a comparison with the previous case we increase the pumping amplitude $a_1 = 34\,\mathrm{ppm}$ to compensate for the drop in the pumping efficiency. Now the idler wave leaks out of the interaction region, and the spin waves cannot be effectively amplified [6]. Therefore, the power of the signal spin wave at the end of the pumping region is more than ten times less than in the oblique SAW case. We want to emphasize that the difference in the spin-wave output comes not from greater parametric coupling with the SAW but from the group velocity of the idler spin wave being zero.

However, in the case of $\phi = 0$ an absolute instability is possible with a threshold acoustic amplitude $a_{\mathrm{th}} \approx 45\,\mathrm{ppm}$ for $L_g = 60\,\mu\mathrm{m}$. After exceeding this threshold, thermal fluctuations are pumped and increase their amplitudes exponentially.

VI. CONCLUSION

We developed a perturbation theory of parametric interaction between localized spin waves and acoustic waves. With the theory we demonstrated that (i) the localization of spin waves modifies the momentum conservation law for parametric pumping, (ii) the symmetry of the magnetoelastic coupling allows an efficient interaction between the Rayleigh surface acoustic waves and forward-volume spin waves with circular precession, and (iii) both convective and absolute parametric instabilities can develop for spin waves under experimentally achievable amplitudes of surface acoustic waves, which results in efficient amplification of spin waves in ferromagnetic waveguides.

ACKNOWLEDGMENTS

The work was supported by the U.S. Defense Advanced Research Projects Agency (DARPA) Signal Processing at RF (SPAR) Grant No. HR0011-17-2-0005.

[1] N. Bloembergen, *Nonlinear Optics*, 4th ed. (World Scientific, Singapore, 1996).

[2] N. S. Erokhin, V. E. Zakharov, and S. S. Moiseev, Second harmonic generation by an electromagnetic wave incident on inhomogeneous plasma, Sov. Phys. JETP **29** No. 1, 101 (1969).

[3] M. Lesieur, *Turbulence in Fluids*, Fluid Mechanics and Its Applications, Vol. 40 (Kluwer Academic Publishers, Dordrecht, The Netherlands, 1997).

[4] V. S. L'Vov, *Wave Turbulence under Parametric Excitation: Applications to Magnets*, Springer Series in Nonlinear Dynamics (Springer-Verlag, Berlin, 1994).

[5] V. E. Zakharov, V. S. L'vov, and G. Falkovich, *Kolmogorov Spectra of Turbulence I: Wave Turbulence*, Springer Series in Nonlinear Dynamics Vol. 1 (Springer-Verlag, Berlin Heidelberg, 1992).

[6] G. A. Melkov, A. A. Serga, V. S. Tiberkevich, Yu. V. Kobljanskij, and A. N. Slavin, Nonadiabatic interaction of a propagating wave packet with localized parametric pumping, Phys. Rev. E **63**, 066607 (2001).

[7] M. Born and E. Wolf, *Principles of Optics: Electromagnetic Theory of Propagation, Interference and Diffraction of Light* (Cambridge University Press, Cambridge, 1999).

[8] H. Matthews and F. R. Morgenthaler, Phonon-Pumped Spin-Wave Instabilities, Phys. Rev. Lett. **13**, 614 (1964).

[9] B. A. Auld and H. Matthews, Parametric traveling-wave acoustic amplification in ferromagnets, J. Appl. Phys. **36**, 3599 (1965).

[10] C. W. Haas, Amplification of spin waves by phonon pumping, J. Phys. Chem. Solids **27**, 1687 (1966).

[11] D. H. Lyons and H. Matthews, Parametric excitation of spin waves by phonon pumping, J. Appl. Phys. **44**, 1348 (1973).

[12] A. G. Gurevich and G. A. Melkov, *Magnetization Oscillations and Waves* (CRC Press, Boca Raton, FL, 1996).

[13] E. Schlömann, J. J. Green, and U. Milano, Recent developments in ferromagnetic resonance at high power levels, J. Appl. Phys. **31**, S386 (1960).

[14] V. V. Zautkin, V. E. Zakharov, V. S. L'Vov, S. L. Musher, and S. S. Starobinets, Parallel spin-wave pumping in yttrium garnet single crystals, Sov. Phys. JETP **35** No. 5, 926 (1972).

[15] G. A. Melkov, A. A. Serga, A. N. Slavin, V. S. Tiberkevich, A. N. Oleinik, and A. V. Bagada, Parametric interaction of magnetostatic waves with a nonstationary local pump, J. Exp. Theor. Phys. **89**, 1189 (1999).

[16] T. Brächer, P. Pirro, and B. Hillebrands, Parallel pumping for magnon spintronics: Amplification and manipulation of magnon spin currents on the micron-scale, Phys. Rep. **699**, 1 (2017).

[17] Yu. V. Kobljanskyj, G. A. Melkov, A. A. Serga, V. S. Tiberkevich, and A. N. Slavin, Effective microwave ferrite convolver using a dielectric resonator, Appl. Phys. Lett. **81**, 1645 (2002).

[18] H. Keshtgar, M. Zareyan, and G. E. W. Bauer, Acoustic parametric pumping of spin waves, Solid State Commun. **198**, 30 (2014).

[19] P. Chowdhury, A. Jander, and P. Dhagat, Nondegenerate parametric pumping of spin waves by acoustic waves, IEEE Magn. Lett. **8**, 1 (2017).

[20] L. Thevenard, I. S. Camara, J.-Y. Prieur, P. Rovillain, A. Lemaître, C. Gourdon, and J.-Y. Duquesne, Strong reduction of the coercivity by a surface acoustic wave in an out-of-plane magnetized epilayer, Phys. Rev. B **93**, 140405(R) (2016).

[21] L. Thevenard, I. S. Camara, S. Majrab, M. Bernard, P. Rovillain, A. Lemaître, C. Gourdon, and J.-Y. Duquesne, Precessional magnetization switching by a surface acoustic wave, Phys. Rev. B **93**, 134430 (2016).

[22] P. Kuszewski, J.-Y. Duquesne, L. Becerra, A. Lemaître, S. Vincent, S. Majrab, F. Margaillan, C. Gourdon, and L. Thevenard, Optical Probing of Rayleigh Wave Driven Magnetoacoustic Resonance, Phys. Rev. Appl. **10**, 034036 (2018).

[23] *Spin Dynamics in Confined Magnetic Structures I*, edited by B. Hillebrands and K. Ounadjela, Topics in Applied Physics Vol. 1 (Springer-Verlag, Berlin, Heidelberg, 2001).

[24] A. A. Serga, A. V. Chumak, and B. Hillebrands, YIG magnonics, J. Phys. D **43**, 264002 (2010).

[25] M. Collet, X. de Milly, O. d'Allivy Kelly, V. V. Naletov, R. Bernard, P. Bortolotti, J. Ben Youssef, V. E. Demidov, S. O. Demokritov, J. L. Prieto *et al.*, Generation of coherent spin-wave modes in yttrium iron garnet microdiscs by spin-orbit torque, Nat. Commun. **7**, 10377 (2016).

[26] C. Safranski, I. Barsukov, H. K. Lee, T. Schneider, A. A. Jara, A. Smith, H. Chang, K. Lenz, J. Lindner, Y. Tserkovnyak *et al.*, Spin caloritronic nano-oscillator, Nat. Commun. **8**, 117 (2017).

[27] Y. Ebata and S. Mitobe, A numerical method for stress analysis in a saw resonator, in *Proceedings of the 1998 IEEE Ultrasonics Symposium Sendai, Japan* (IEEE Press, Piscataway, NJ), pp. 257–260.

[28] C. Kittel, Interaction of spin waves and ultrasonic waves in ferromagnetic crystals, Phys. Rev. **110**, 836 (1958).

[29] R. L. Comstock and B. A. Auld, Parametric coupling of the magnetization and strain in a ferrimagnet. I. parametric excitation of magnetostatic and elastic modes, J. Appl. Phys. **34**, 1461 (1963).

[30] O. Dzyapko, I. Lisenkov, P. Nowik-Boltyk, V. E. Demidov, S. O. Demokritov, B. Koene, A. Kirilyuk, T. Rasing,

V. Tiberkevich, and A. Slavin, Magnon-magnon interactions in a room-temperature magnonic Bose-Einstein condensate, Phys. Rev. B **96**, 064438 (2017).

[31] I. Lisenkov, V. Tyberkevych, S. Nikitov, and A. Slavin, Theoretical formalism for collective spin-wave edge excitations in arrays of dipolarly interacting magnetic nanodots, Phys. Rev. B **93**, 214441 (2016).

[32] R. Verba, G. Melkov, V. Tiberkevich, and A. Slavin, Collective spin-wave excitations in a two-dimensional array of coupled magnetic nanodots, Phys. Rev. B **85**, 014427 (2012).

[33] R. Verba, V. Tiberkevich, and A. Slavin, Damping of linear spin-wave modes in magnetic nanostructures: Local, nonlocal, and coordinate-dependent damping, Phys. Rev. B **98**, 104408 (2018).

[34] X. Li, D. Labanowski, S. Salahuddin, and C. S. Lynch, Spin wave generation by surface acoustic waves, J. Appl. Phys. **122**, 043904 (2017).

[35] A. Barra, A. Mal, G. Carman, and A. Sepulveda, Voltage induced mechanical/spin wave propagation over long distances, Appl. Phys. Lett. **110**, 072401 (2017).

[36] R. Verba, I. Lisenkov, I. Krivorotov, V. Tiberkevich, and A. Slavin, Nonreciprocal Surface Acoustic Waves in Multilayers with Magnetoelastic and Interfacial Dzyaloshinskii-Moriya Interactions, Phys. Rev. Appl. **9**, 064014 (2018).

[37] J. Jorzick, S. O. Demokritov, B. Hillebrands, M. Bailleul, C. Fermon, K. Y. Guslienko, A. N. Slavin, D. V. Berkov, and N. L. Gorn, Spin Wave Wells in Nonellipsoidal Micrometer Size Magnetic Elements, Phys. Rev. Lett. **88**, 047204 (2002).

[38] K. Y. Guslienko, R. W. Chantrell, and A. N. Slavin, Dipolar localization of quantized spin-wave modes in thin rectangular magnetic elements, Phys. Rev. B **68**, 024422 (2003).

[39] C. Bayer, J. Jorzick, B. Hillebrands, S. O. Demokritov, R. Kouba, R. Bozinoski, A. N. Slavin, K. Y. Guslienko, D. V. Berkov, N. L. Gorn *et al.*, Spin-wave excitations in finite rectangular elements of $Ni_{80}Fe_{20}$, Phys. Rev. B **72**, 064427 (2005).

[40] R. Verba, M. Carpentieri, G. Finocchio, V. Tiberkevich, and A. Slavin, Excitation of propagating spin waves in ferromagnetic nanowires by microwave voltage-controlled magnetic anisotropy, Sci. Rep. **6**, 25018 (2016).

[41] R. Verba, M. Carpentieri, G. Finocchio, V. Tiberkevich, and A. Slavin, Excitation of Spin Waves in an In-Plane-Magnetized Ferromagnetic Nanowire Using Voltage-Controlled Magnetic Anisotropy, Phys. Rev. Appl. **7**, 064023 (2017).

[42] S. Klingler, A. V. Chumak, T. Mewes, B. Khodadadi, C. Mewes, C. Dubs, O. Surzhenko, B. Hillebrands, and A. Conca, Measurements of the exchange stiffness of YIG films using broadband ferromagnetic resonance techniques, J. Phys. D **48**, 015001 (2014).

[43] B. A. Auld, *Acoustic Fields and Waves in Solids* (John Wiley & Sons, NY, 1973).

[44] M. Weiler, L. Dreher, C. Heeg, H. Huebl, R. Gross, M. S. Brandt, and S. T. B. Goennenwein, Elastically Driven Ferromagnetic Resonance in Nickel Thin Films, Phys. Rev. Lett. **106**, 117601 (2011).

[45] P. G. Gowtham, T. Moriyama, D. C. Ralph, and R. A. Buhrman, Traveling surface spin-wave resonance spectroscopy using surface acoustic waves, J. Appl. Phys. **118**, 233910 (2015).

[46] J. Janušonis, C. L. Chang, T. Jansma, A. Gatilova, V. S. Vlasov, A. M. Lomonosov, V. V. Temnov, and R. I. Tobey, Ultrafast magnetoelastic probing of surface acoustic transients, Phys. Rev. B **94**, 024415 (2016).

[47] C. L. Chang, A. M. Lomonosov, J. Janusonis, V. S. Vlasov, V. V. Temnov, and R. I. Tobey, Parametric frequency mixing in a magnetoelastically driven linear ferromagnetic-resonance oscillator, Phys. Rev. B **95**, 060409(R) (2017).

[48] V. V. Temnov, C. Klieber, K. A. Nelson, T. Thomay, V. Knittel, A. Leitenstorfer, D. Makarov, M. Albrecht, and R. Bratschitsch, Femtosecond nonlinear ultrasonics in gold probed with ultrashort surface plasmons, Nat. Commun. **4**, 1468 (2013).

[49] R. Verba, V. Tiberkevich, and A. Slavin, Influence of interfacial Dzyaloshinskii-Moriya interaction on the parametric amplification of spin waves, Appl. Phys. Lett. **107**, 112402 (2015).

[50] P. Pirro, T. Brächer, A. V. Chumak, B. Lägel, C. Dubs, O. Surzhenko, P. Görnert, B. Leven, and B. Hillebrands, Spin-wave excitation and propagation in microstructured waveguides of yttrium iron garnet/Pt bilayers, Appl. Phys. Lett. **104**, 012402 (2014).

[51] A. Vansteenkiste, J. Leliaert, M. Dvornik, M. Helsen, F. Garcia-Sanchez, and B. Van Waeyenberge, The design and verification of MuMax3, AIP Adv. **4**, 107133 (2014).